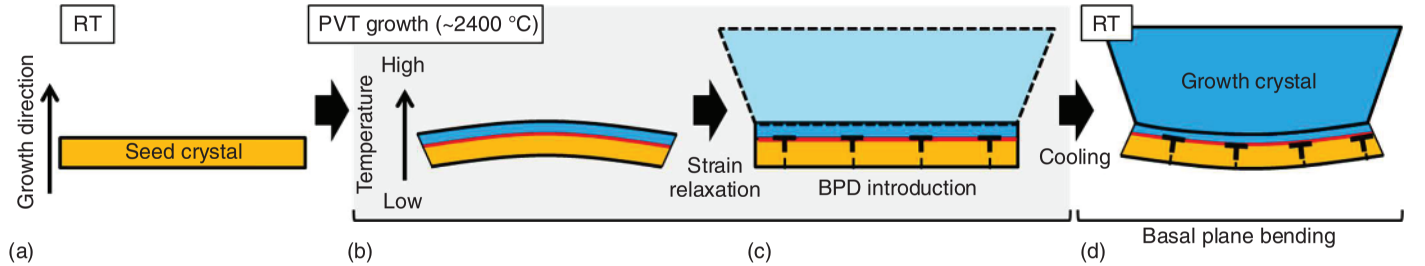

Figure 1.19 Schematic of introduction of BPDs at grown-crystal/seed interface during PVT growth process, and the resulting basal plane bending after the growth process. Source: Shioura et al. [39]. © 2019, Elsevier; (a) seed crystal prior to PVT growth, (b) basal plane bending associated the large temperature gradient at the initial stage of growth, which occurs in a convex manner toward the growth direction, (c) introduction of BPDs to relax the misfit strain within the basal plane at the grown-crystal/seed interface, and (d) concave-shape basal plane bending toward the growth direction after cooling to room temperature.

misfit strain within the basal plane at the grown-crystal/seed interface, and (d) the resultant concave-shaped basal plane bending in the growth direction after PVT growth. The large basal plane bending due to the poor heat dissipation in the initial stage of PVT growth of SiC was observed experimentally by Hock et al. using in situ X-ray diffraction [46]. They found that the degree of basal plane bending increased with the growth rate, implying that the latent heating due to the condensation of source gas species plays an important role in the basal plane bending in the initial stage of PVT growth.

The final concave shape of the basal plane in the growth direction shown in Figure 1.19d is consistent with the lattice bending observed by HRXRD, and thus, the large positive temperature gradient established at the growing crystal surface during the initial stage of PVT growth would be the most plausible cause of the observed BPD networks. The relationship between the observed BPD networks and the formation of threading dislocations in the initial stage of PVT growth [10–12] is yet to be clarified. However, in Figure 1.17, in addition to the BPD networks, dot-like features are also observed at the nodes of the BPD networks. They are likely to correspond to threading dislocations and suggest that the BPD networks are related closely to them and would be an important source of threading dislocations in PVT-grown 4H-SiC crystals.

As revealed in Figure 1.16, the BPD networks extended fairly deeply in the seed crystal. The maximum depth of the networks in the seed crystal can be estimated from their positions on the surface of the 1.5° off-oriented $(000\bar{1})$ wafer; the networks extended up to 7 mm on the wafer surface from the grown-crystal/seed interface toward the backside of the seed crystal. The distance of 7 mm on the wafer surface corresponds to a depth of 300 μm from the grown-crystal/seed interface toward the backside of the seed crystal. In the initial stage of PVT growth, growth islands are likely to nucleate on the seed crystal surface and then coalesce as the crystal growth proceeds (see Figure 1.18b). Under a large positive temperature gradient, the growth islands tend to incorporate BPDs to relieve the misfit strain due to the temperature gradient, and when the islands coalesce, the BPDs are rearranged and form networks at the grown-crystal/seed interface. The results obtained by Shioura et al. indicated that these BPD networks at the interface were accompanied by extra half-planes pointing toward the backside of the seed crystal and caused the (0001) basal plane to bend in a concave manner in the growth direction after the PVT growth process [39]. An important question here is how and why these BPD networks migrated into the seed crystal during PVT growth.

There are two possible mechanisms for the migration of the BPD networks into the seed crystal, namely, (i) the glide motion of BPDs on the basal plane and (ii) the climb motion of BPDs across the basal plane. To clarify the mechanism for BPD migration into the seed crystal during PVT growth, Shioura et al. conducted a masked PVT growth experiment on a 4° off-oriented $(000\bar{1})$ seed crystal [39]. The result is shown in Figure 1.20, where a reflection X-ray topograph for the diffraction condition $\boldsymbol{g} = 11\bar{2}\bar{8}$ acquired from the boundary area between the masked and unmasked regions of the seed crystal is shown. The masked region (right-hand side of the figure) was covered with a graphite plate during PVT growth to prevent

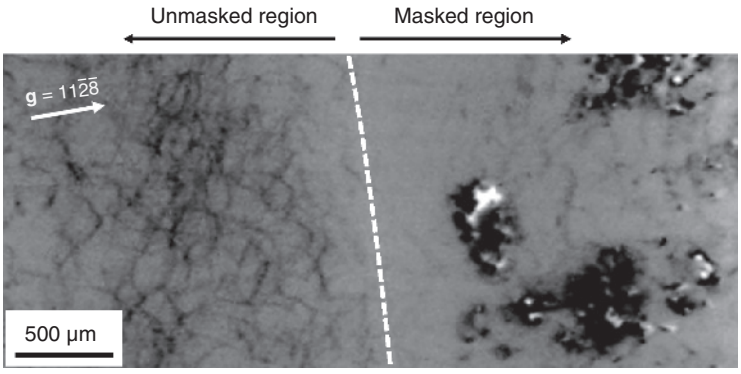

Figure 1.20 Enlarged reflection X-ray topograph for diffraction condition $\boldsymbol{g} = 11\bar{2}\bar{8}$ acquired from the boundary area between the masked and unmasked regions of the seed crystal; the 4H-SiC crystal was grown on the unmasked region (left-hand side of the dashed line in the topograph), whereas no crystal growth occurred on the masked region (right-hand side of the dashed line). The topograph shows clearly that the BPD networks in the seed crystal existed only in the unmasked region of the seed crystal. Source: Shioura et al. [39].

crystal growth. As shown in the figure, BPD networks exist only in the unmasked region and do not extend into the masked region. This result shows clearly that the observed BPD networks migrated into the seed crystal through the climb motion of dislocations, as schematically illustrated in Figure 1.21, rather than the glide motion. This is because, had the glide motion been the dominant mechanism for BPD migration, then the BPD networks formed during the initial stage of PVT growth should have glided on the basal plane into the masked region beyond the boundary between the unmasked and masked regions and then been observed in the masked region of the seed crystal after the crystal growth.

The climb motion of dislocations is driven by the injection, diffusion, and incorporation of intrinsic point defects, such as vacancies and interstitials, to the dislocations [47]. As described in Section 1.3.3, the observed BPD networks were accompanied by extra half-planes pointing toward the backside of the seed crystal, and thus, their migration toward the backside of the seed crystal requires vacancies to be incorporated in the dislocations as illustrated schematically in Figure 1.20. Given the migration depth of the BPD networks, it is clear that a large number of vacancies were injected during the initial stage of PVT growth. The mechanism for this remains unclear, but the poor dissipation of the latent heat in the initial stage of PVT growth (see Figure 1.18b,d) would cause local heating of the growing crystal surface, which may induce the injection of a large number of vacancies into the growing crystal.

1.4 Conclusions

SiC is a promising material for the next generation of power semiconductor devices, and the adoption of SiC power devices is critical for enabling faster, smaller, lighter,

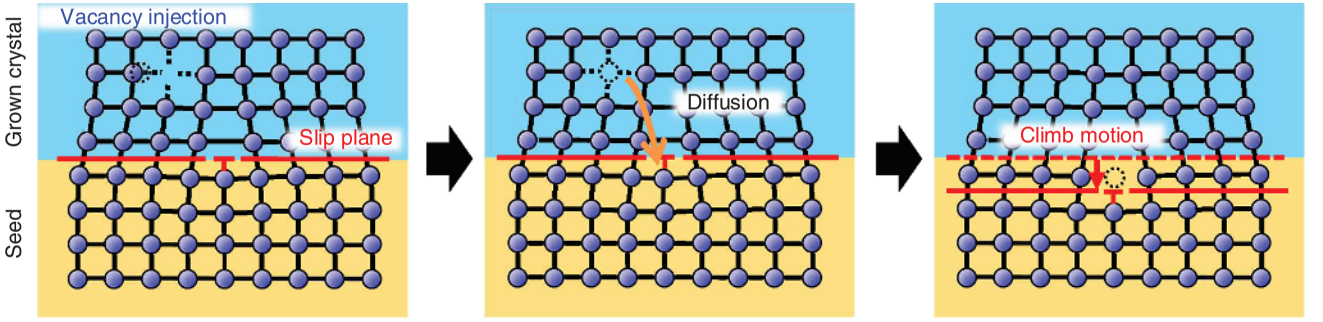

Figure 1.21 Schematic of the climb motion of a BPD toward the backside of the seed crystal due to the vacancy injection into the growing crystal during PVT growth. Source: Shioura et al. [39]. © 2019, Elsevier.

and more powerful power electronic systems. However, it is amply clear that such a successful adoption of SiC power devices for a wide range of power electronics systems relies considerably on establishing the manufacturing technology for large-diameter high-quality SiC single crystals. This chapter described recent progress in understanding the dislocation formation processes in PVT-grown SiC crystals, which is essential for obtaining high-quality SiC crystals.

After a brief introduction (Section 1.1), Section 1.2 was dedicated to understanding the BPD nucleation and multiplication processes during the PVT growth of 4H-SiC crystals. A large number of BPDs are introduced from the shoulder region of the growth front of 4H-SiC crystals, where a large thermoelastic shear stress is thought to be imposed during PVT growth. Detailed investigations of the BPD distribution in grown crystals suggest that BPDs nucleated at the shoulder region of a growing crystal largely determine the BPD distribution across the entire crystal.

In Section 1.3, the defect structure at the grown-crystal/seed interface of PVT-grown 4H-SiC crystals was investigated using 4H-SiC wafers with a beveled interface between the grown crystal and seed crystal. The existence of BPD networks at the grown-crystal/seed interface was revealed, and they extended considerably into the seed crystal. Such networks were likely to be caused by a large positive temperature gradient imposed on the growing crystal surface because of the local heating by the latent heat dissipation associated with the condensation of Si- and C-bearing species from the vapor during the initial stage of PVT growth. It was also revealed by masked-growth experiments that the migration of the BPD networks deep into the seed crystal was caused by the injection of a large number of vacancies during the initial stage of PVT growth of 4H-SiC crystals.

References

1 Kimoto, T. and Cooper, J.A. (2014). *Fundamentals of Silicon Carbide Technology: Growth, Characterization, Devices, and Applications*. Singapore: Wiley.
2 Tairov, Yu.M. and Tsvetkov, V.F. (1978). *J. Cryst. Growth* 43: 209.
3 Wahab, Q., Ellison, A., Henry, A. et al. (2000). *Appl. Phys. Lett.* 76: 2725.
4 Fujiwara, H., Naruoka, H., Konishi, M. et al. (2012). *Appl. Phys. Lett.* 100: 242102.
5 Yamamoto, K., Nagaya, M., Watanabe, H. et al. (2012). *Mater. Sci. Forum* 717–720: 477.
6 Agarwal, A., Fatima, H., Haney, S., and Sei-Hyung, R. (2007). *IEEE Electron Device Lett.* 28: 587.
7 Veliadis, V., Hearne, H., Stewart, E.J. et al. (2012). *IEEE Electron Device Lett.* 33: 952.
8 Bergman, P., Lendenmann, H., Nilsson, P.A. et al. (2001). *Mater. Sci. Forum* 353–356: 299.
9 Lendenmann, H., Dahquist, F., Johansson, N. et al. (2001). *Mater. Sci. Forum* 353–356: 727.
10 Takahashi, J., Ohtani, N., and Kanaya, M. (1996). *J. Cryst. Growth* 167: 596.

11 Sanchez, E.K., Liu, J.Q., De Graef, M. et al. (2002). *J. Appl. Phys.* 91: 1143.
12 Suo, H., Tsukimoto, S., Eto, K. et al. (2018). *Jpn. J. Appl. Phys.* 57: 065501.
13 Hobgood, H.McD, Brady, M.F., Brixius, W.H. et al. (2000). *Mater. Sci. Forum* 338–342: 3.
14 Selder, M., Kadinski, L., Durst, F., and Hofmann, D. (2001). *J. Cryst. Growth* 226: 501.
15 Ma, R.-H., Zhang, H., Dudley, M., and Prasad, V. (2003). *J. Cryst. Growth* 258: 318.
16 Gao, B. and Kakimoto, T. (2014). *Cryst. Growth Des.* 14: 1272.
17 Herro, Z.G., Epelbaum, B.M., Bickermann, M. et al. (2004). *J. Cryst. Growth* 262: 105.
18 Yamaguchi, T., Ohtomo, K., Sato, S. et al. (2015). *J. Cryst. Growth* 431: 24.
19 Pons, M., Madar, R., and Billon, T. (2003). *Silicon Carbide – Recent Major Advances* (eds. W.J. Choyke, H. Matsunami and G. Pensl), 121–136. Berlin: Springer.
20 Powell, A.R., Leonard, R.T., Brady, M.F. et al. (2004). *Mater. Sci. Forum* 457–460: 41.
21 Tymicki, E., Grasza, K., Diduszko, R. et al. (2007). *Cryst. Res. Technol.* 42: 1232.
22 Ohtani, N., Ohshige, C., Katsuno, M. et al. (2014). *J. Cryst. Growth* 386: 9.
23 Ohshige, C., Takahashi, T., Ohtani, N. et al. (2014). *J. Cryst. Growth* 408: 1.
24 Tani, K., Fujimoto, T., Kamei, K. et al. (2016). *Mater. Sci. Forum* 858: 73.
25 Straubinger, T.L., Bickermann, M., Weingärtner, R. et al. (2002). *J. Cryst. Growth* 240: 117.
26 Nakano, T., Shinagawa, N., Yabu, M., and Ohtani, N. (2019). *J. Cryst. Growth* 516: 51.
27 Sonoda, M., Nakano, T., Shioura, K. et al. (2018). *J. Cryst. Growth* 499: 24.
28 Wang, S., Dudley, M., Carter, C. Jr., et al. (1993). *Mater. Res. Soc. Symp. Proc.* 307: 249.
29 Zhang, X., Ha, S., Hanlumnyang, Y. et al. (2007). *J. Appl. Phys.* 101: 053517.
30 Hirth, J.P. and Lothe, J. (1982). *Theory of Dislocations*, 2e, 63. New York: Wiley.
31 Ha, S., Mieszkowski, M., Skowronski, M., and Rowland, L.B. (2002). *J. Cryst. Growth* 244: 257.
32 Ohtani, N., Katsuno, M., Tsuge, H. et al. (2006). *Jpn. J. Appl. Phys.* 45: 1738.
33 Powell, A.R., Sumakeris, J.J., Khlebnikov, Y. et al. (2016). *Mater. Sci. Forum* 858: 5.
34 Nakashima, S. and Harima, H. (1997). *Phys. Status Solidi A* 162: 39.
35 Sugie, R. and Uchida, T. (2017). *J. Appl. Phys.* 122: 195703.
36 Sakakima, H., Takamoto, S., Murakami, Y. et al. (2018). *Jpn. J. Appl. Phys.* 57: 106602.
37 Ohtani, N., Katsuno, M., Fujimoto, T. et al. (2009). *Jpn. J. Appl. Phys.* 48: 065503.
38 Chen, Y., Dhanaraj, G., Dudley, M. et al. (2006). *Mater. Res. Soc. Symp. Proc.* 911: 151.
39 Shioura, K., Shinagawa, N., Izawa, T., and Ohtani, N. (2019). *J. Cryst. Growth* 515: 58.
40 Yugami, H., Nakashima, S., Mitsuishi, A. et al. (1987). *J. Appl. Phys.* 61: 354.

41 Nakashima, S., Harima, H., Ohtani, N., and Katsuno, M. (2004). *J. Appl. Phys.* 95: 3547.
42 Matsumoto, T., Nishizawa, S., and Yamasaki, S. (2010). *Mater. Sci. Forum* 645–648: 247.
43 Sasaki, S., Suda, J., and Kimoto, T. (2012). *Mater. Sci. Forum* 717–720: 481.
44 Drowart, J., de Maria, G., and Inghram, M.G. (1958). *J. Chem. Phys.* 29: 1015.
45 Dold, P. (2015). *Advances in Photovoltaics: Part 4, Semiconductors and Semimetals*, vol. 92 (eds. G.P. Willeke and E.R. Weber), 13. Waltham, MA: Academic Press.
46 Hock, R., Konias, K., Perdicaro, L. et al. (2010). *Mater. Sci. Forum* 645–648: 29.
47 Hull, D. and Bacon, D.J. (1984). *Introduction to Dislocations*, 3e, 58. Oxford: Pergamon Press.